PCCP

Accepted Manuscript

ROYAL SOCIETY OF CHEMISTRY

www.rsc.org/pccp

ARTICLE TYPE www. rsc.org/xxxxxx | XXXXXXXX

Low-energy vibrational spectra of flexible diphenyl molecules: Biphenyl, Diphenylmethane, Bibenzyl and 2-, 3- and 4-Phenyltoluene

M. A. Martin-Drumel,*[a,b]‡ O. Pirali,[a,b] C. Falvo,[a] P. Parneix,[a] A. Gamboa,[a] F. Calvo[c] and Ph. Bréchignac[a]

Received Xth XXXXXXXXXX 20XX, Accepted Xth XXXXXXXXX 20XX
First published on the web Xth XXXXXXXXXX 200X
DOI: 10.1039/b000000x

Abstract: Gas phase absorption far-infrared (FIR) spectra of six flexible hydrocarbon molecules containing two phenyl groups –biphenyl, diphenylmethane, bibenzyl and 2-, 3-, 4-phenyltoluene– are reported for the first time, allowing an accurate determination of most of their active low-frequency vibrational modes. DFT calculations have been carried out at the harmonic and perturbative anharmonic levels to predict the vibrational spectra of these molecules and unambiguously assign observed vibrational modes.

1 Introduction

Unidentified infrared bands (UIBs) observed in a wide variety of astrophysical environments[1,2] are suspected to originate from polycyclic aromatic hydrocarbons (PAHs) emission bands, and are thus often refered to as aromatic infrared bands (AIBs). In consequence PAHs have been the subject of extensive experimental and theoretical studies that have mostly supported this hypothesis although no individual PAH molecule could be identified to date. Recently, new investigations on these compounds have focused on the far-infrared (FIR) spectral region where vibrational modes are more molecule-specific, as they correspond to skeletal vibrations, than mid-infrared (MIR) ones.[3–7]

Theoretical modeling of the spectra of carbon stars does not yet include the possible presence of polyphenyl-type molecules (i.e. non-aromatic molecules containing aromatic rings) together with PAHs compounds.[8] However, laboratory experiments have recently shown that polyphenyls such as biphenyl or terphenyls are predominant products of reactions involving phenyls radicals in presence of benzene.[9] Such compounds could thus play an active role in the formation of carbonaceous aromatic molecules and their detection might explain some mechanisms in PAHs formation. In this context the possible detection of low-frequency vibrations of these molecules by instruments such as Herschel or SOFIA appears promising.

The low-frequency vibrational spectra of gas phase naphthalene, the simplest two-ring PAH, and of some of its aromatic derivatives (quinoline, isoquinoline and azulene) have recently been investigated.[5,6] It is now worth while and timely to focus on polyphenyl molecules having closely related molecular structures.

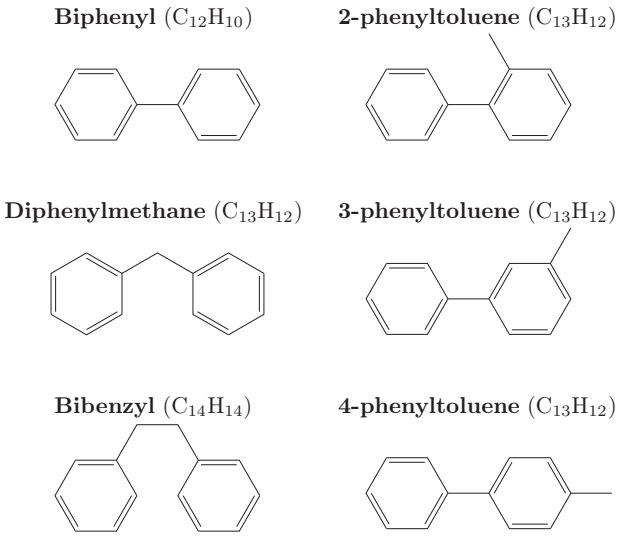

Fig. 1 Chemical structure of the six molecules studied in this work.

Six non-rigid molecules containing two aromatic rings have been chosen for their structural similarity: biphenyl, diphenylmethane, bibenzyl and 2-, 3-, 4-phenyltoluene (see figure 1). Determination of geometrical parameters of these compounds has been the subject of numerous investigations since the 60s, mainly through their study in the condensed phase (*vide in-*

[a] *Institut des Sciences Moléculaires d'Orsay (ISMO), CNRS, Université Paris-Sud , bât. 210, 91405 Orsay Cedex, France. Tel: +331 69 35 97 65; E-mail: mmartin@cfa.harvard.edu*
[b] *SOLEIL Synchrotron, L'orme des Merisiers, Saint-Aubin, 91192 Gif-Sur-Yvette, France*
[c] *Laboratoire Interdisciplinaire de Physique (LIPhy), Grenoble, France*
‡ Present address: Harvard-Smithsonian Center for Astrophysics, 60 Garden Street, 02138 Cambridge MA, USA

fra). So far, gas phase investigations of these compounds have been limited to the MIR spectral range. However, due to the structural similarity of these compounds, these MIR spectra are also very much alike, preventing from any individual identification.[10] Investigation of their low-lying vibrational modes thus appears as an efficient way to discriminate among them. Furthermore, FIR is a valuable spectral region to study the influence on the vibrational frequencies specific to the interphenyl bridge and the methyl susbstituent.[11]

In the present article we report gas-phase investigations of the FIR spectra of these six flexible bichromophores. Experimental band positions have been unambiguously assigned using DFT calculations including anharmonic corrections. In the course of this study, we noticed that no assignment of MIR bands to specific vibrational modes was available for these molecules. We thus also propose partial assignments of their MIR spectra as a complement to earlier publications (see references below).

2 Methods

2.1 Samples

All the samples are commercial in the condensed phase and have been purchased from Sigma-Aldrich. They present purity higher than 98% and have been used without further purification.

2.2 Infrared measurements

Gas phase FIR spectra have been investigated at room temperature at the AILES beamline of the SOLEIL synchrotron using a Bruker IFS125 FT-interferometer, a multipass White-type cell and a globar source. Owing to the 150 m absorption path length, we have been able to detect vibrational signatures of the different molecules at pressures of a few µbar. The cell and the interferometer were separated by polypropylene windows. We used a 4.2 K bolometer detector and a Mylar beamsplitter of 6 µm thickness. For all compounds, a MIR absorption spectrum has also been recorded (ZnSe windows, KBr beamsplitter and MCT detector). All spectra have been obtained at 0.5 cm^{-1} resolution and are composed of 1000 scans of transmission and 1000 scans of reference. In all figures, the measured spectra are presented in absorbance.

Below 400 cm^{-1}, the signal-to-noise ratio is relatively limited by both weak intensity of low-frequency vibrational modes and strong residual water lines. Thus the spectra presented in that range have been smoothed for the sake of clarity. Weak vibrational modes below 50 cm^{-1} could not be observed using this technique. Furthermore, at the spectral resolution used the rotational contour of the vibrational bands is observed for some vibrational bands where P-, Q- and R-branches can be distinguished. In that case, frequencies of vibrational modes have been taken at the maximum of absorbance for the bands presenting a Q-branch, and at the minimum of absorbance between P- and R-branches for *b*-type bands. When the rotational contour of the band is not observed, frequencies of vibrational modes have been taken at the maximum of absorbance of the considered mode. With this approach, we estimate the uncertainty on the band centers to be better than 2 cm^{-1}.

2.3 Theoretical approach

Quantum chemical calculations have been performed at the level of density-functional theory (DFT) using the hybrid B3LYP and B97-1 functionals, as well as MP2 Møller-Plesset post-Hartree-Fock level, with the various basis sets 6-31G(d), 6-311G(d,p), and cc-pVTZ. All calculations were carried out with the Gaussian09 software package,[12] including molecular optimization, harmonic and anharmonic vibrational analyses. They were run on the SOLEIL local cluster using 24 or 48 processors. For the sake of comparison, the indicated CPU times are those reported on the output files. Infrared spectra were simulated for the electronic ground state with an arbitrary bandwidth of 2 cm^{-1} in order to be compared with the experimental spectra (with no consideration for the rotational P-, Q-, R-contours).

Recently, the B97-1/6-311G(d,p) method was shown to be particularly suitable for predicting the vibrational spectra of aromatic naphthalene derivatives.[6] We first have ascertained the performance of this approach for the presently studied molecules by comparing it to various other methods in the case of biphenyl. The best method, as designated based on the quality of experimental agreement and the computational cost, was then applied to all other investigated molecules.

The agreement between experimental and calculated frequencies can be quantified by the relative difference $\delta = (\tilde{\nu}_{\mathrm{calc}} - \tilde{\nu}_{\mathrm{exp}})/\tilde{\nu}_{\mathrm{exp}}$ where $\tilde{\nu}_{\mathrm{calc}}$ and $\tilde{\nu}_{\mathrm{exp}}$ are the calculated and measured frequencies of a given vibrational mode at a specific computational level. For frequencies higher than 650 cm^{-1}, only assigned bands are reported in the tables, the complete list of calculated modes being supplied as suplementary material. The systematization of the results, considering the vibrational modes, has been made in terms of Mean Absolute Error (MAE), and maximum and minimum absolute discrepancies. These values evaluating the good quality of the results are reported in the different tables.

3 Results

3.1 Biphenyl

Biphenyl has been the subject of numerous spectroscopic investigations due to its conformational peculiarities: while the molecule is planar under normal conditions of temperature and pressure in the crystalline state, it becomes twisted in the liquid and gas phases (figure 2). Gas-phase spectroscopy of this molecule has been investigated from the THz to the UV ranges by electron diffraction,[13] jet-cooled electronic excitation,[14] UV and infrared absorption,[10,15,16] and Raman infrared techniques.[17] The angle θ between the two cycles has been studied both from the experimental ($\theta = 45 \pm 10°$ through electron diffraction measurements[13]) and theoretical ($\theta \sim 40$–$43°$[15]) perspectives. To our knowledge, the low-frequency vibrational modes of biphenyl have only been investigated in the crystalline phase so far.[18]

In the gas phase, biphenyl in its lowest-energy conformation belongs to the D_2 point group. Several axial orientations are suitable following Mulliken's convention. In agreement with the work of Beenken and Lischka[19] we have chosen an axial orientation as shown in figure 2: the z axis corresponds to minimum inertia while the x axis maximizes inertia. With these notations the vibrational modes of biphenyl can be classified as:

$$\Gamma = 15\mathrm{A} + 13\mathrm{B}_1 + 16\mathrm{B}_2 + 16\mathrm{B}_3.$$

In the infrared, active modes are of B_1, B_2 or B_3 symmetry.

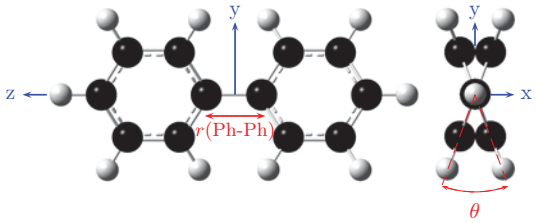

Fig. 2 Geometry of biphenyl molecule and axes definition. r(Ph–Ph) is the bond length of the central C–C bond (Ph refers to a phenyl group) and θ is the twist angle.

The geometry of the molecule has been optimized with four computational methods, namely B3LYP/6-311G(d,p), B97-1/6-311G(d,p), B97-1/cc-pVTZ, and MP2/cc-pVTZ. Table 1 shows the results obtained for the optimal twist angle θ and the C–C bond length r(Ph–Ph). The different results are relatively close to each other and also agree with the literature.[13,15] The vibrational frequencies were then determined for these optimized geometries. Anharmonic frequencies could be determined using vibrational perturbation theory within DFT, however this approach turned out to be unfeasible at the MP2 level, hence only harmonic data are reported. The results obtained with these methods are compared with experimental data in figures 3, 4 and in table 2. With the exception of weak ν_{57}, ν_{41} and ν_{43} modes, all expected vibrational modes can be assigned in the FIR spectrum. The weakness of ν_{57} allows the unambiguous assignment of ν_{27}, despite the proximity of the two modes. On the MIR spectrum, 11 vibrational bands are also assigned.

Table 1 Optimized geometrical parameters of biphenyl obtained from several quantum chemical methods. Values of the twist angle θ taken from the literature are also given.

Method	r(Ph–Ph)/Å	θ/°
B3LYP/6-311G(d,p)	1.48	40.42
B97-1/6-311G(d,p)	1.49	40.12
B97-1/cc-pVTZ	1.49	38.61
MP2/cc-pVTZ	1.47	39.87
Experimental (Bastiansen[13])		45 ± 10
Theory (Suzuki[15])		40–43

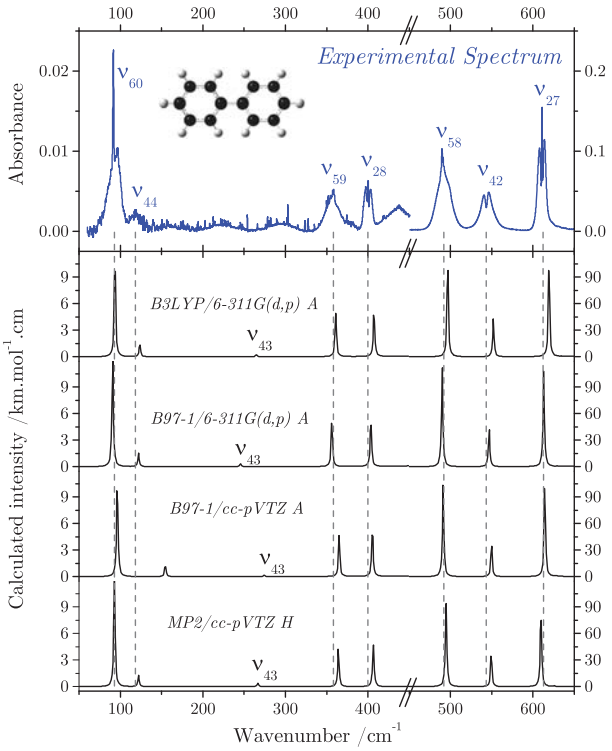

Fig. 3 FIR absorption spectrum of biphenyl and comparison with theoretical calculations. Below 450 cm^{-1}, intensities have been scaled by one order of magnitude for the sake of clarity. *A* and *H* refer to anharmonic and harmonic frequency determinations, respectively.

We first compare the performances of the B3LYP and B97-

Table 2 Experimental vibrational modes of biphenyl and comparison with different harmonic (H) and anharmonic (A) quantum chemical calculations.

Sym.	Exp.	B3LYP/6-311G(d,p)				B97-1/6-311G(d,p)				B97-1/cc-pVTZ				MP2/cc-pVTZ			Assign.
		H	A	δ	I	H	A	δ	I	H	A	δ	I	H	δ^b	I	
	/cm^{-1}	/cm^{-1}	/cm^{-1}	/%	^{a}	/cm^{-1}	/cm^{-1}	/%	^{a}	/cm^{-1}	/cm^{-1}	/%	^{a}	/cm^{-1}	/%		
A		65	61		0.0	67	34		0.0	67	66		0.0	70		0	ν_{15}
B3	92	95	94	2.2	0.9	94	91	-1.1	0.9	94	96	4.3	0.8	93	1.1	0.9	ν_{60}
B2	118	126	124	5.1	0.1	125	122	3.4	0.1	126	155	31.4	0.1	122	3.4	0.09	ν_{44}
B2		268	265		0.02	267	246		0.03	266	274		0.01	267		0.03	ν_{43}
A		313	309		0.0	311	305		0.0	311	323		0.0	311		0	ν_{14}
B3	358	368	361	0.8	0.4	366	356	-0.6	0.4	369	365	2.0	0.3	364	1.7	0.3	ν_{59}
B1	401	414	407	1.5	0.4	410	404	0.7	0.4	412	405	1.0	0.4	407	1.5	0.4	ν_{28}
A		420	413		0.0	417	402		0.0	419	412		0.0	414		0	ν_{13}
B3	490	503	497	1.4	7.9	499	490	0.0	8.1	498	491	0.2	7.5	495	1.0	7.5	ν_{58}
B2	544	559	552	1.5	3.1	555	547	0.6	3.2	557	550	1.1	2.7	549	0.9	2.8	ν_{42}
B1	611	626	619	1.3	7.7	620	613	0.3	7.8	619	614	0.5	7.6	610	-0.2	6.3	ν_{27}
B3		629	622		0.01	623	616		0.0	623	616		0.0	614		0.01	ν_{57}
B2		641	634		0.02	635	629		0.03	636	629		0.06	626		0.06	ν_{41}
B3	699	716	709	1.4	63.3	713	701	0.3	58.3	716	708	1.3	58.4	699	0.0	26.8	ν_{56}
B3	738	756	747	1.2	71.2	752	740	0.3	81.8	755	747	1.2	71.3	747	1.2	103.9	ν_{55}
B2	779	798	787	1.0	6.4	793	780	0.1	7.0	798	789	1.3	6.4	786	0.9	9.2	ν_{39}
B1	966	981	972	0.6	0.7	976	961	-0.5	0.7	984	975	0.9	0.8	965	-0.1	0.7	ν_{25}
B1	1013	1026	1011	-0.2	6.6	1019	1004	-0.9	6.9	1023	1007	-0.6	6.8	1021	0.8	8.1	ν_{23}
B1	1046	1067	1048	0.2	3.2	1062	1034	-1.1	3.4	1063	1049	0.3	2.7	1065	1.8	3.1	ν_{22}
B2	1075	1101	1078	0.3	8.3	1096	1065	-0.9	8.7	1097	1099	2.2	7.8	1098	2.1	8.2	ν_{36}
B1	1178	1202	1183	0.4	0.4	1197	1165	-1.1	0.4	1199	1188	0.8	0.4	1196	1.5	0.8	ν_{21}
B2	1436	1462	1439	0.2	8.9	1454	1428	-0.6	9.0	1458	1432	-0.3	8.1	1482	3.2	4.0	ν_{32}
B1	1488	1516	1488	0.0	33.2	1508	1472	-1.1	32.6	1512	1489	0.1	31.8	1507	1.3	29.2	ν_{20}
B1	1601	1646	1603	0.1	12.1	1639	1597	-0.2	12.2	1638	1598	-0.2	13.4	1643	2.6	8.0	ν_{19}
CPU^c /h		2	453			2	456			14	3532			3006			
MAE^d /%				1.08				0.77				2.76			1.41		
Max^e /%				5.1				3.4				31.4			3.4		
Min^e /%				0.0				0.0				0.1			0.0		

^{a} I /km.mol^{-1}, ^{b} Determinated using calculated harmonic frequencies, ^{c} CPU time, ^{d} Mean Absolute Error, ^{e} Maximumm and minimum discrepancies

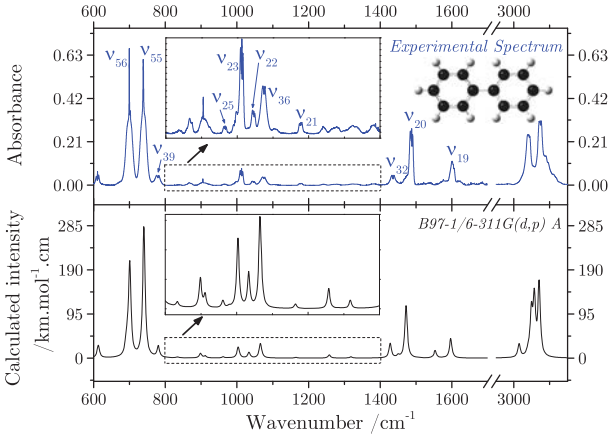

Fig. 4 MIR absorption spectrum of biphenyl and comparison with anharmonic calculations at the B97-1/6-311G(d,p) level.

1 functionals with the same 6-311G(d,p) basis set. For the two methods, the computing times provided by the Gaussian09 software are comparable to each other but the B97-1 functional yields FIR anharmonic frequencies closer to the experimental values and to a lower MAE value (table 2). We note that in the MIR region, results obtained with the B3LYP functional are slighly closer to the experimental values, however since the emphasis of this work is on the lowest frequency modes we do prefer the results obtained using the B97-1 functional. Anharmonic calculations using this functional were repeated with a larger basis set, cc-pVTZ. Again, the results are in good agreement with experimental data with the exception of the ν_{44} mode for which the calculated wavenumber is far from the experimental measurement. We thus conclude that the B97-1/cc-pVTZ method does not perform significantly better in combined terms of chemical accuracy and computational cost. Harmonic vibrational frequencies obtained with the MP2/cc-pVTZ method are very computationally expensive, but show a good agreement with experimental FIR measurements. However, the vibrational modes predicted at the harmonic level in the MIR range are at significant variance with the measurements and it would be interesting to perform

anharmonic calculations with this same method once they become computationally affordable. On a side note, we notice that the estimation of the anharmonic frequencies using empirical correction factors, as commonly used in the literature for the MIR range (see for example Talbi and Chandler [8]) has not been performed since this method is less reliable for FIR vibrations. Low-lying vibrational modes appear less affected by anharmonicities of the potential energy surface than the higher-lying modes, resulting in non-unique or ambiguous correction factors in the entire IR region.

In addition, we have also performed calculations at the MP2/6-311G(d,p) level, which was suggested to be suitable for geometry optimization of naphthalene, a molecule rather close to biphenyl.[20] In our case, such a calculation gave harmonic frequencies in large disagreement with our experimental results. As a consequence, we decided not to pursue further with this method for this type of molecules.

The present study shows that DFT performs well for predicting vibrational frequencies of biphenyl in agreement with experimental spectra. In particular, the B97-1/6-311G(d,p) method appears particularly accurate with a reasonable computational cost, making it our method of choice for the other molecules studied in this work.

3.2 Diphenylmethane

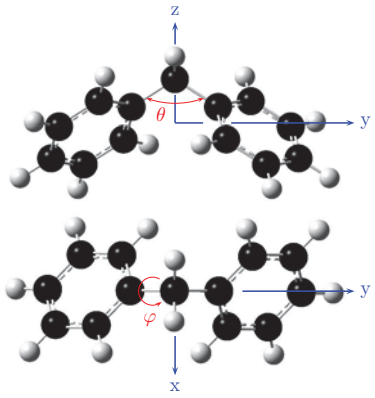

Fig. 5 Geometry of diphenylmethane. θ is the bending angle between the central C–CH_2–C bonds and φ is the dihedral angle between one phenyl group and the plane defined by the central C–CH_2–C bonds.

Figure 5 shows the geometrical structure of the diphenylmethane molecule characterized by two equivalent dihedral angles φ_1 and φ_2 and one bending angle θ.

Diphenylmethane has been previously studied by IR, Raman and UV techniques in the solid and liquid phases.[21–24] In the gas phase, the UV spectrum has been documented[25] but no data about the IR spectrum are available. Recently, the association of vibrationally- and rotationally-resolved UV and Fourier-transform microwave spectroscopies has provided accurate values of ground state rotational constants of the molecule.[26] The determination of dihedral angles has also been the subject of theoretical investigations yielding $\theta \sim 114°$ and $\varphi \sim 57°$.[26]

Diphenylmethane belongs to the C_2 point group symmetry and has 69 normal vibrational modes, all IR active:

$$\Gamma = 35\mathrm{A} + 34\mathrm{B}.$$

The experimental FIR spectrum of diphenylmethane is shown in fig. 6. The similarity of our calculated values ($\theta \sim 114°$ and $\varphi \sim 51°$, optimizations at the B97-1/6-311G(d,p) level of theory) with the angles fitted by Stearns *et al.*[26] makes us confident on the quality of the potential energy surface described with this approach.

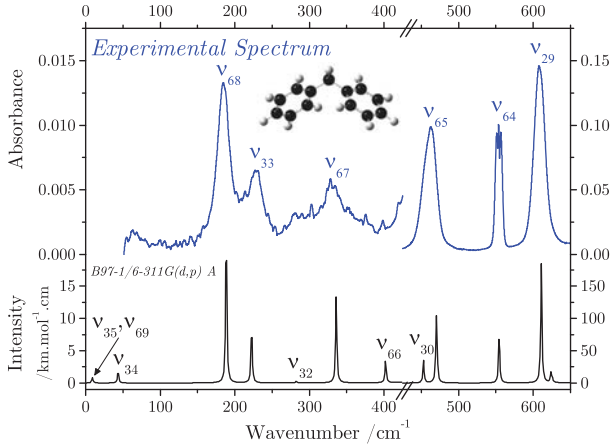

Fig. 6 FIR absorption spectrum of diphenymethane compared with calculated anharmonic spectrum obtained at the B97-1/6-311G(d,p) level of theory. The intensities of the modes lying below 400 cm^{-1}, refered to on the left scale, have been magnified by 10 compared to the upper part of the spectrum.

Harmonic and anharmonic frequencies of diphenylmethane have been calculated at the same level. The simulated spectrum (fig. 6, bottom panel) is in very good agreement with the experimental spectrum presently measured, allowing the assignment of FIR vibrational modes. Table 3 summarizes the experimental and calculated vibrational modes of diphenylmethane. Weak modes could not be assigned on the spectrum. The very low dispersion of the δ parameter again confirms the quality of the anharmonic calculation. Note the presence of three very low frequency modes falling out of the range of the present experimental data.

Table 3 Vibrational modes of diphenylmethane. Comparison of experimental values with theoretical data obtained at the harmonic (H) and anharmonic (A) B97-1/6-311G(d,p) levels.

Sym.	Exp.	B97-1/6-311G(d,p)				Assign.
		H	A	δ	I	
	/cm^{-1}	/cm^{-1}	/cm^{-1}	/%	/km.mol^{-1}	
B		18	9		0.06	ν_{69}
A		21	9		0.01	ν_{35}
A		64	43		0.13	ν_{34}
B	185	192	189	1.9	1.70	ν_{68}
A	229	224	223	-2.8	0.63	ν_{33}
A		287	282		0.02	ν_{32}
B	330	337	336	1.8	0.96	ν_{67}
B		411	402		0.24	ν_{66}
A		412	404		0.01	ν_{31}
A		459	453		2.50	ν_{30}
B	463	477	470	1.6	8.25	ν_{65}
B	554	560	554	0.1	5.29	ν_{64}
A	608	619	611	0.5	13.48	ν_{29}
A		630	624		1.13	ν_{28}
B		632	626		0.36	ν_{63}
B	698	710	697	-0.1	27.32	ν_{62}
A	698	713	700	0.3	41.39	ν_{27}
B	736	747	734	-0.2	51.69	ν_{61}
A	736	748	737	0.2	20.55	ν_{26}
A	816	827	815	-0.2	2.45	ν_{25}
B	893	899	884	-1.0	3.84	ν_{58}
B	1004	1012	998	-0.6	1.05	ν_{54}
B	1032	1047	1029	-0.3	8.85	ν_{53}
B	1077	1102	1076	-0.1	11.07	ν_{52}
A	1184	1199	1181	-0.2	1.06	ν_{15}
B	1203	1216	1190	-1.1	2.31	ν_{49}
A	1455	1484	1451	-0.3	12.17	ν_{10}
B	1499	1519	1488	-0.7	24.54	ν_{44}
B	1606	1638	1599	-0.4	14.25	ν_{42}
B	2857	3053	2914	2.0	11.58	ν_{41}
A	2926	3017	2937	0.4	25.86	ν_6
CPU /h		3	655			
MAE /%				0.76		
Max /%				2.8		
Min /%				0.1		

3.3 Bibenzyl

The most stable conformation of bibenzyl (1,2-diphenylethane, see fig. 7) has been debated for decades, as experimental and theoretical works have remained inconclusive.[27,28] This molecule was found to be present in the *anti* (antiperiplanar, see fig. 7) form in the crystal state[29,30] while in the liquid state, both *anti* and *gauche* (synclinal) forms are present.[31] A single gas-phase study based on electron diffraction[32] has shown that the molecule is present under *anti* conformation although the presence of the *gauche* form could not be excluded. To date, no conclusive structural results have been reported on the *gauche* conformer, which is only assumed to belong to the C_2 point group.[29] In the *anti* form bibenzyl is of C_{2h} symmetry. In these two groups, the 78 vibrational modes of the molecule can be classified as

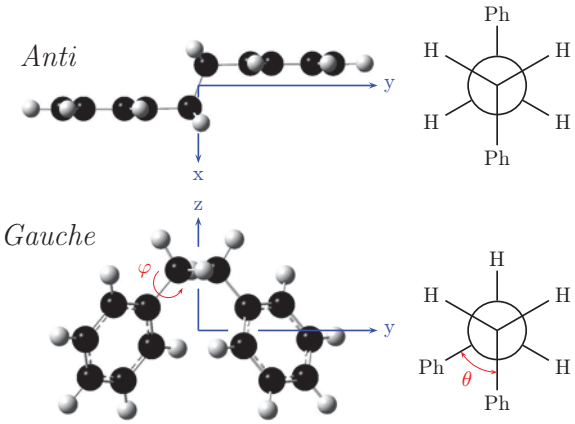

Fig. 7 Representation and Newman projection of bibenzyl molecule in the *anti* and *gauche* configurations. The two phenyl (Ph) groups belong to parallel planes for the *anti* conformer. For the *gauche* conformer, φ is the torsional angle between the phenyl group and the plane defined by the central C-CH_2–CH_2 bond, and θ is the dihedral angle between the two phenyl groups.

follows:

$$\Gamma_{anti} = 22A_g + 18A_u + 17B_g + 21B_u$$
$$\Gamma_{gauche} = 40A + 38B$$

For the *anti* conformation, only A_u and B_u symmetries are IR active while all modes are active in the *gauche* form.

Experimental spectra of bibenzyl have been recorded in both MIR and FIR spectral regions (figure 8) and we have determined anharmonic frequencies of the two conformers using the B97-1/6-311G(d,p) method (tables 4 and 5). In the case of the *anti* conformer, one negative anharmonic frequency was obtained for the ν_{40} mode. This highly anharmonic mode corresponds to the rotation of the two phenyl groups along the C–CH_2 bonds; the induced deformation is sketched in figure 9. We tried to improve the anharmonic frequency determination by increasing the size of the integrals or using other methods (as B3LYP), but all these attempts gave the same result, thereby questioning the validity of the perturbative treatment of anharmonicities. Therefore, and despite the good agreement of calculated anharmonic frequencies with the experimental spectrum in the MIR range, we have decided to compare experimental values to the harmonic calculation in the FIR range.

In the MIR range, the vibrational bands of *anti* and *gauche* conformers are too close from each other to allow an unambiguous assignment with the exception of one band at 1345 cm^{-1}, which appears to be specific to the *gauche* conformer (ν_{12} mode, see fig. 8). In contrast, in the FIR range the calculated spectrum of the two conformers differs signif-

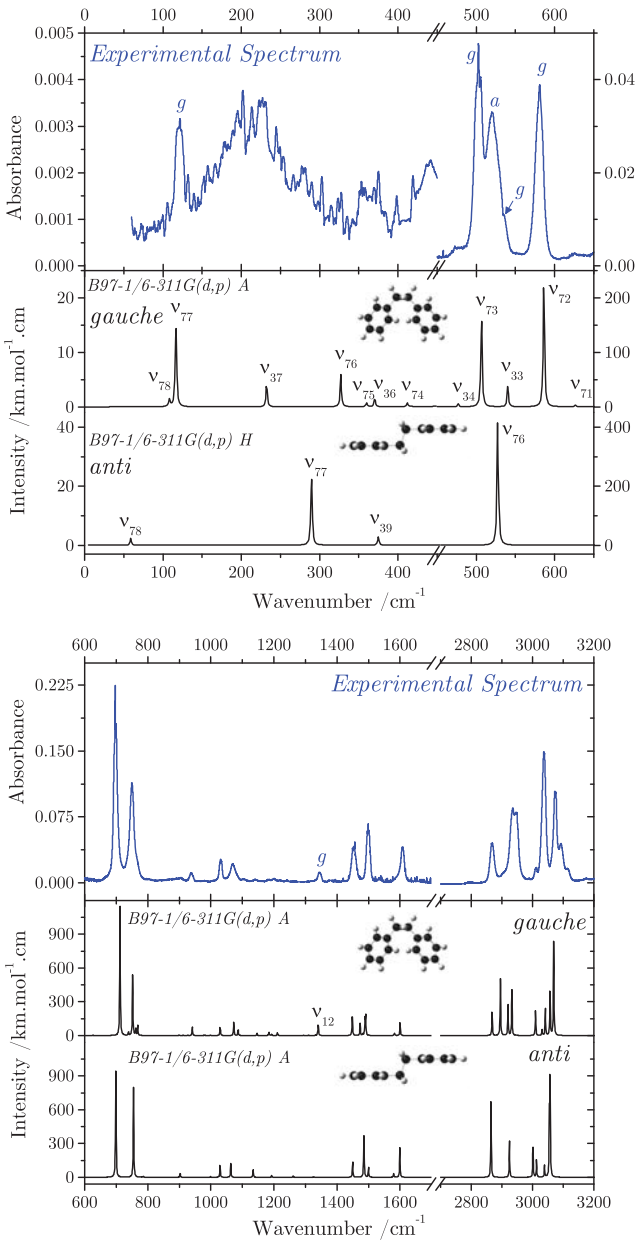

Fig. 8 FIR (upper part) and MIR (lower part) experimental spectra (blue line) of bibenzyl and comparison with B97-1/6-311G(d,p) DFT calculations (black line) for *gauche* (anharmonic calculation) and *anti* (harmonic calculation) conformations. Below 450 cm^{-1}, the intensities have been magnified by a factor 10.

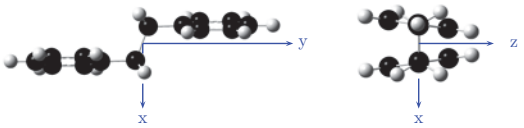

Fig. 9 Anharmonic deformation induced by the ν_{40} vibrational mode of bibenzyl in *anti* conformation.

Table 4 Vibrational modes of bibenzyl in its *gauche* conformation. Comparison of experimental and calculated (obtained at the harmonic (H) and anharmonic (A) B97-1/6-311G(d,p) levels) spectra.

Sym.	Exp.	B97-1/6-311G(d,p)				Assign.
		H	A	δ	I	
	/cm^{-1}	/cm^{-1}	/cm^{-1}	/%	/km.mol^{-1}	
A		29	38		0	ν_{40}
A		47	105		0.01	ν_{39}
B		28	108		0.10	ν_{78}
B	121	122	117	-3.7	1.20	ν_{77}
A		119	117		0.03	ν_{38}
A		228	232		0.31	ν_{37}
B		323	327		0.43	ν_{76}
B		362	360		0.05	ν_{75}
A		367	370		0.11	ν_{36}
B		411	412		0.05	ν_{74}
A		412	417		0.01	ν_{35}
A		483	477		0.40	ν_{34}
B	503	511	507	0.7	13.09	ν_{73}
A		543	540		2.81	ν_{33}
B	581	587	586	0.9	16.96	ν_{72}
B		631	626		0.23	ν_{71}
A		631	627		0.04	ν_{32}
B	697	711	712	2.2	76.90	ν_{70}
B	750	765	752	0.3	41.60	ν_{69}
B	938	949	941	0.3	5.55	ν_{65}
A	1031	1047	1031	0.0	2.54	ν_{21}
B	1071	1089	1073	0.2	9.03	ν_{60}
B	1345	1365	1340	-0.3	7.72	ν_{53}
B	1453	1477	1449	-0.3	10.19	ν_{52}
A	1499	1520	1489	-0.7	10.02	ν_{10}
B	1499	1521	1491	-0.5	12.16	ν_{50}
B	1608	1641	1600	-0.5	7.03	ν_{48}
CPU /h		3	1186			
MAE /%				0.82		
Max /%				3.7		
Min /%				0.0		

icantly. Three bands belonging to the *gauche* conformer can be identified on the spectrum, attesting the presence of this conformer in the gas phase. The band at 520 cm^{-1} cannot be assigned to the *gauche* conformer and appears to correspond to the ν_{76} mode of the *anti* form. Based on these results, we can attest for the first time the *gauche* conformer to be present in the gas phase together with the *anti* form (although only a single band of this conformer can be assigned with confidence). Based on the intensity of the bands at 520 cm^{-1} and 581 cm^{-1} (chosen for the absence of rotational contour) we estimate the *gauche*:*anti* ratio to be equal to 2:1 (66% *gauche* and 33% *anti*).

This ratio can also be evaluated from statistical mechanics considerations, the population p_g and p_a in the *gauche*(g) or *anti*(a) conformers being approximated by the ratio of the cor-

Table 5 Vibrational modes of bibenzyl in its *anti* conformation. Comparison of experimental spectrum with calculated spectrum obtained at the harmonic (H) and anharmonic (A) B97-1/6-311G(d,p) levels.

Sym.	Exp.	B97-1/6-311G(d,p)				Assign.
		H	δ_H	A	I	
	/cm^{-1}	/cm^{-1}	/%	/cm^{-1}	/km.mol^{-1}	
Au		21		*	0	ν_{40}
Au		35		15	0.01	ν_{39}
Bg		54		30	0	ν_{57}
Bu		61		54	0.16	ν_{78}
Ag		119		109	0	ν_{22}
Ag		235		230	0	ν_{21}
Bu		290		285	1.86	ν_{77}
Bg		313		312	0	ν_{56}
Au		369		370	0.21	ν_{38}
Bg		411		403	0	ν_{55}
Au		412		403	0	ν_{37}
Ag		478		468	0	ν_{20}
Bu		532		522	3.34	ν_{75}
Bu	520	529	1.7	524	30.51	ν_{76}
Ag		621		612	0	ν_{19}
Bg		631		624	0	ν_{54}
Au		633		626	0.03	ν_{36}
Bu	697	713	0.2	699	80.26	ν_{74}
Bu	750	770	0.7	755	58.05	ν_{73}
Bu	905	920	-0.3	902	2.85	ν_{71}
Bu	1031	1046	-0.2	1029	8.68	ν_{68}
Au	1071	1084	-0.7	1063	8.80	ν_{32}
Au	1142	1157	-0.7	1134	5.26	ν_{31}
Au	1453	1476	-0.2	1450	10.56	ν_{27}
Bu	1499	1520	-0.9	1485	30.97	ν_{64}
Bu	1608	1641	-0.6	1599	19.53	ν_{62}
CPU /h		3		1041		
MAE /%			0.62			
Max /%			1.7			
Min /%			0.2			

* Mode with a negative calculated anharmonic frequency

responding quantum partition functions Z_g and Z_a,

$$p_g(T) = \frac{Z_g(T)}{Z_a(T) + Z_g(T)}. \quad (1)$$

Within the harmonic approximation, the quantum partition function Z_α, $\alpha = g$ or a, is written as

$$Z_\alpha(T) = g_\alpha e^{-\beta E_\alpha} \prod_{i=1}^{\kappa} \frac{e^{-\beta\hbar\omega_i^{(\alpha)}/2}}{1 - e^{-\beta\hbar\omega_i^{(\alpha)}}} \quad (2)$$

where E_α is the minimum electronic energy of conformer α, $\kappa = 78$ is the total number of vibrational frequencies, $\omega_i^{(\alpha)}$ is the harmonic frequencies of mode i and g_α is a degeneracy factor accounting for the number of equivalent isomers by permutation-inversion symmetry. Since the *anti* and *gauche* conformers belong to the C_{2h} and C_2 point groups, respectively, $g_g/g_a = 2$. Based on our electronic structure calculations, Eqs. (1) and (2) can be solved to estimate the populations of the *anti* and *gauche* conformers as a continuous function of temperature.

At the B97-1/6-311G(d,p) level of theory the *anti* conformer is lower in energy than *gauche* conformer by about 126 cm^{-1} therefore at 0 K all molecules lie in the *anti* conformer. However at $T = 300$ K both conformers are found to coexist with a *gauche*:*anti* ratio equal to 1:2, in semi-quantitative agreement with the experimental estimate based on IR intensities ratio. Although these simple calculations confirm the coexistence between the isomers, they cannot explain the measurements with a significant accuracy. We can speculate about this relative disagreement as being caused by several possible sources. First, it is unclear whether the B97-1 method used here is sufficiently accurate to describe polyphenyl molecules. In particular, dispersion could increase the energetic stability of the *gauche* conformer with respect to the *anti* conformer and therefore increase its population at room temperature. Preliminary calculations using the wB97xD functional actually indicate a good agreement for the harmonic frequencies relative to the B97-1 calculations. However, as was the case for the B97-1 and B3LYP calculations, the perturbative vibrational approximation appears unsufficient as the ν_{40} torsional mode remains unphysical (negative) with this dispersion-corrected functional. Because anharmonicities also impact the thermal populations, it is thus necessary to evaluate them using nonperturbative approaches such as molecular dynamics, an issue lying beyond the present effort. Finally, it should be kept in mind that the 2:1 ratio from calculated IR intensities has to be taken cautiously, because IR intensities are notoriously difficult to predict accurately. Additional efforts necessary to address this interesting issue will be reported in a subsequent dedicated study.

As a final note for this molecule, a broad contribution can be seen around 200 cm^{-1} on the experimental spectrum. This signature could correspond to the merging of the vibrational modes of both conformers predicted in the 200–350 cm^{-1} range. It could also be related to the ν_{40} mode of the *anti* conformer , as a result from a cumulative effect of hot bands originating from a manifold set of thermally populated levels, associated with the large amplitude torsional motion of the two phenyl groups (see figure 9).

3.4 2-, 3-, 4-phenyltoluene

The compounds 2-, 3-, 4-phenyltoluene are respectively ortho, meta and para CH_3-substituted biphenyls. These molecules do not have any specific symmetry (all belong to the C_1 point group) and have 69 vibrational modes. To our best knowledge, no spectroscopic study has been previously reported for these molecules.

The FIR absorption spectra of 2-, 3-, and 4-phenyltoluene

recorded in this work are presented in figure 10. The simulated spectra obtained using B97-1/6-311G(d,p) harmonic and anharmonic calculations are also presented in the bottom part of each spectrum.

Table 6 Vibrational modes of 2-phenyltoluene. Comparison of experimental values with theoretical data obtained at the harmonic (H) and anharmonic (A) levels.

Exp.	B97-1/6-311G(d.p)					Assign.
	H	δ_H	A	δ_A	I	
/cm^{-1}	/cm^{-1}	/%	/cm^{-1}	/%	/km.mol^{-1}	
	131		*		0.25	ν_{69}
	43		118		0.05	ν_{68}
90	87	-3.5	84	-6.7	0.45	ν_{67}
	103		107		0.13	ν_{66}
189	194	2.9	65	-65.7	1.64	ν_{65}
259	264	2.1	187	-27.8	0.30	ν_{64}
290	294	1.3	287	-0.9	0.46	ν_{63}
323	328	1.5	284	-11.9	0.71	ν_{62}
403	406	0.8	321	-20.3	0.91	ν_{61}
	413		405		0.38	ν_{60}
452	463	2.4	439	-2.9	5.24	ν_{59}
517	520	0.6	513	-0.8	4.43	ν_{58}
	554		546		1.42	ν_{57}
560	570	1.8	570	1.8	3.16	ν_{56}
620	627	1.1	622	0.3	2.99	ν_{55}
620	631	1.9	626	0.9	2.76	ν_{54}
701	713	1.7	743	6.1	40.41	ν_{53}
727	738	1.5	718	-1.2	7.08	ν_{51}
753	760	0.9	750	-0.4	65.79	ν_{50}
913	928	1.6	972	6.5	2.10	ν_{45}
942	953	1.2	942	0.0	0.59	ν_{44}
998	1002	0.4	796	-20.2	1.49	ν_{40}
1013	1019	0.6	1002	-1.1	8.88	ν_{38}
1073	1095	2.0	1096	2.1	5.18	ν_{34}
1159	1180	1.8	1165	0.5	0.25	ν_{31}
1180	1197	1.4	1215	2.9	0.30	ν_{30}
1242	1284	3.4	1251	0.7	1.19	ν_{28}
1272	1291	1.5	1266	-0.5	1.35	ν_{27}
1388	1410	1.6	1288	-7.2	1.92	ν_{23}
1483	1507	1.6	1453	-2.0	32.70	ν_{18}
1604	1637	2.1	1597	-0.4	3.69	ν_{14}
CPU /h	4		673			
MAE /%		1.66		7.38		
Min /%		3.5		65.7		
Max /%		0.4		0.0		

For these three molecules, our calculation with the B97-1/6-311G(d,p) method poorly reproduces the CH_3-group rotation, as expected for such a hindered rotor motion with a low barrier. This mode is found to have a negative frequency at the anharmonic perturbative level while the harmonic band, although positive by construction, does not correspond to any experimental band. This again confirms the unreliability of the harmonic DFT approximation for such modes associated with nearly free rotations.[33] Despite those unsurprising limitations, the present results are in sufficiently good agreement for all other vibrational modes to allow an unambiguous as-

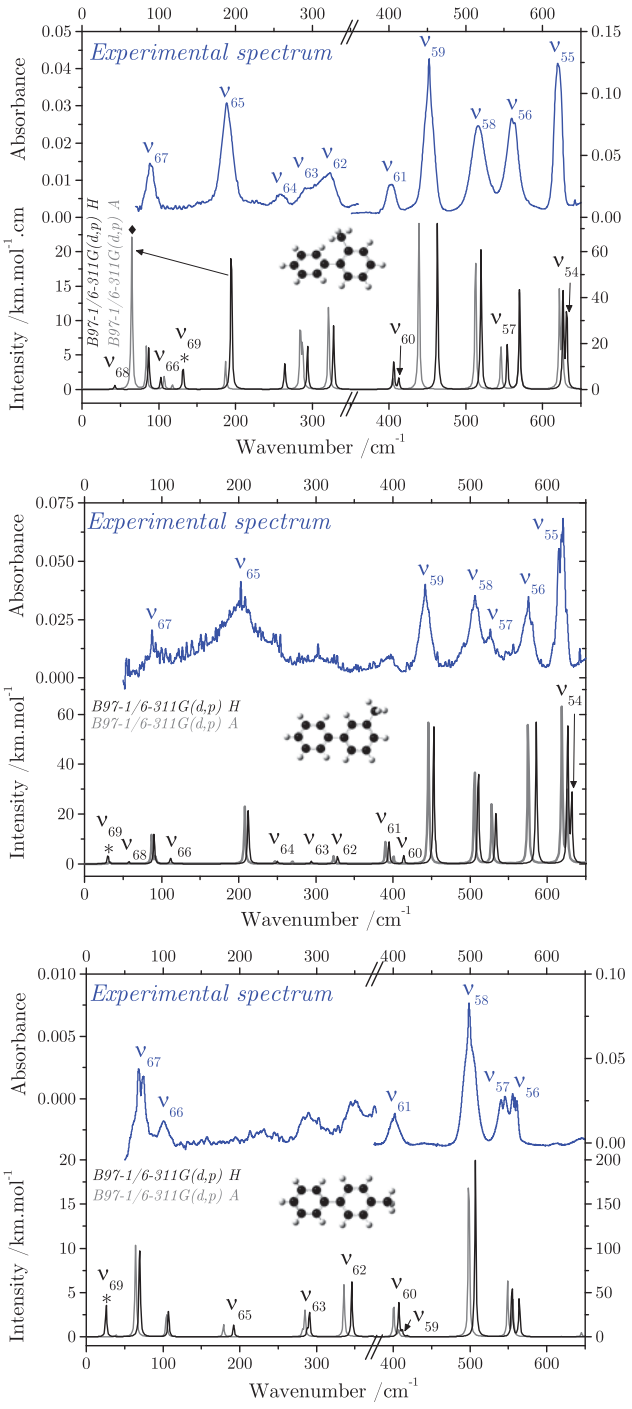

Fig. 10 FIR absorption spectra (blue lines) of 2-, 3-, and 4-phenyltoluene (from top to bottom) and comparison with harmonic (H, black line) and anharmonic (A, gray line) B97-1/6-311G(d,p) calculations.

Table 7 Vibrational modes of 3-phenyltoluene. Comparison of experimental values with theoretical data obtained at the harmonic (H) and anharmonic (A) levels.

Exp.	B97-1/6-311G(d.p)					Assign.
	H	δ_H	A	δ_A	I	
/cm^{-1}	/cm^{-1}	/%	/cm^{-1}	/%	/km.mol^{-1}	
	30		*		0.28	ν_{69}
	58		33		0.06	ν_{68}
88	90	2.4	87	-0.9	0.87	ν_{67}
	112		92		0.19	ν_{66}
203	212	4.6	208	2.4	1.75	ν_{65}
	250		247		0.08	ν_{64}
	294		270		0.08	ν_{63}
	328		323		0.23	ν_{62}
	395		390		0.69	ν_{61}
	414		401		0.24	ν_{60}
442	453	2.4	446	0.9	4.11	ν_{59}
507	511	0.7	506	-0.3	3.01	ν_{58}
527	533	1.2	528	0.2	1.81	ν_{57}
576	586	1.7	575	-0.1	4.29	ν_{56}
618	627	1.4	619	0.1	4.56	ν_{55}
623	632	1.4	626	0.5	2.06	ν_{54}
700	711	1.6	690	-1.4	31.85	ν_{53}
754	767	1.7	753	-0.2	67.44	ν_{50}
791	804	1.6	789	-0.2	11.64	ν_{49}
1394	1436	3.0	1402	0.6	4.39	ν_{22}
1437	1472	2.4	1440	0.2	4.84	ν_{21}
1457	1486	2.0	1456	-0.1	7.28	ν_{20}
1486	1508	1.5	1469	-1.1	34.64	ν_{18}
1608	1640	2.0	1601	-0.4	27.81	ν_{13}
CPU /h	4		639			
MAE /%		1.98		0.60		
Min /%		4.6		2.4		
Max /%		0.7		0.1		

Table 8 Vibrational modes of 4-phenyltoluene. Comparison of experimental values with theoretical data obtained at the harmonic (H) and anharmonic (A) levels.

Exp.	B97-1/6-311G(d.p)					Assign.
	H	δ_H	A	δ_A	I	
/cm^{-1}	/cm^{-1}	/%	/cm^{-1}	/%	/km.mol^{-1}	
	26		*		0.26	ν_{69}
	67		39		0.01	ν_{68}
71	70	-2.0	64	-9.4	0.83	ν_{67}
101	107	6.0	105	3.6	0.21	ν_{66}
	192		179		0.10	ν_{65}
	288		282		0.05	ν_{64}
	291		285		0.21	ν_{63}
	346		336		0.45	ν_{62}
402	407	1.3	401	-0.4	2.88	ν_{61}
	418		401		0.07	ν_{60}
	412		407		0.52	ν_{59}
499	507	1.6	498	-0.1	14.53	ν_{58}
543	555	2.1	549	1.1	4.48	ν_{57}
559	564	0.9	556	-0.6	3.23	ν_{56}
	628		619		0.02	ν_{55}
698	711	1.9	700	0.3	36.58	ν_{53}
758	771	1.7	763	0.6	57.63	ν_{50}
823	836	1.5	819	-0.5	23.66	ν_{48}
1013	1054	4.1	1038	2.4	13.43	ν_{35}
1493	1514	1.4	1473	-1.3	39.27	ν_{19}
1521	1544	1.5	1501	-1.3	9.88	ν_{17}
1576	1595	1.2	1560	-1.0	2.78	ν_{16}
1608	1638	1.9	1593	-0.9	10.19	ν_{14}
CPU /h	4		630			
MAE /%		2.08		1.68		
Min /%		6		9.4		
Max /%		0.9		0.1		

signment of most FIR bands. The observed and calculated frequencies of FIR modes are presented in tables 6, 7 and 8. Here all δ values were calculated using harmonic data as reference. Considering the unphysical numerical value of the CH_3 torsional mode, it was decided to arbitrary label it ν_{69} (lower frequency mode). A star identifier is also used in figure 10 and tables 6, 7, 8 for this specific mode.

3.4.1 2-phenyltoluene The simulated spectrum obtained from the harmonic calculation is in good agreement with the experimental spectrum, with the exception of the ν_{69} mode, the same for which the calculated anharmonic frequency is negative. For the anharmonic calculation, we also note that all vibrations involving the displacement of the methyl group out of the plane of its closest phenyl group are poorly reproduced (see for example the ν_{65} mode labelled with a diamond in figure 10) leading to a high value for the MAE. However, the results obtained with the harmonic calculation allow assigning most of the intense FIR modes of this molecule, except the ν_{69} mode which probably lies below 50 cm^{-1}. In the case of ν_{60} and ν_{61} with similar calculated frequencies, as well as ν_{54} and ν_{55}, the experimental bands were assigned based on calculated intensities.

3.4.2 3-phenyltoluene For 3-phenyltoluene the simulated spectra obtained from both the harmonic and anharmonic calculations are in good agreement with the experimental spectrum. The comparison with DFT calculation allows the assignment of most low-frequency vibrational modes of 3-phenyltoluene, with the exception of six weak modes. Furthermore, at the resolution used here, it was not possible to observe the ν_{55} and ν_{54} modes independently from each other. Since ν_{55} was predicted to be the most intense, we have chosen to assign the experimental value to this mode.

3.4.3 4-phenyltoluene As for 3-phenyltoluene, harmonic and anharmonic calculations for 4-phenyltoluene are in good agreement, again with the exception of ν_{69} mode. Six FIR modes can be assigned by comparison with these calculations. We notice a possible contribution of ν_{62} and ν_{63} modes to the experimental spectrum but, due to the weak signal-to-noise ratio and the non-compensation of the baseline, their assignment remains ambiguous.

4 Discussion

As a result of the influence of the increasing size of the bridge between the two phenyl rings or of the position of the methyl substituant, the FIR spectra of biphenyl, diphenylmethane, bibenzyl and 2-, 3- and 4-phenyltoluene are relatively different, allowing some characterization of these molecules based on their vibrational properties. In the case of biphenyl, diphenylmethane and bibenzyl, three strong absorption bands lie in the spectral range 450–650 cm^{-1} while below 450 cm^{-1}positions and intensities of the different vibration modes are significantly different. 2- and 3-phenyltoluene present relatively similar FIR spectra in position and intensity, unlike 4-phenyltoluene.

In the following part, we further discuss the influence of the molecular structure on several common vibrational modes. We have first compared three vibrational modes of biphenyl with the corresponding modes of naphthalene, as taken from Pirali *et al.* [5]

4.1 Evolution of low-frequency vibrational modes from naphthalene to biphenyl

Among the molecules studied in this work, biphenyl is the one having its molecular structure closest to naphthalene. We thus have selected three FIR vibrational modes, one out-of-plane ("butterfly") and two in-plane ("scissors" and "antisymmetric stretching") vibrations, all chosen for their unambiguous identification to skeletal deformations, to be compared for the two molecules. Figure 11 shows a schematic representation of the deformation induced by the three selected vibrations together with their influence on the band position. The relative frequency change induced by the structural modification was evaluated by the parameter Δ expressed for the vibrational mode $\tilde{\nu}_i^{\mathrm{B}}$ of biphenyl as $\Delta_i = (\tilde{\nu}_i^{\mathrm{B}} - \tilde{\nu}_i^{\mathrm{N}})/\tilde{\nu}_i^{\mathrm{N}}$ where $\tilde{\nu}_i^{\mathrm{N}}$ is the frequency of the corresponding mode of naphthalene, taken from the work of Pirali *et al.* [5] We note that the presence of a C–C bond between the two phenyl groups induces a significant decrease of the butterfly and antisymmetric stretching frequencies by comparison to naphthalene, as a consequence of the decrease in the rigidity of the molecule concomitant with the decrease in the number of bonding π orbitals. However, the frequencies of the antisymmetric stretching mode for the two molecules are very close, which was expected since this mode corresponds to the deformation of the carbon skeleton, itself similar for the two molecules.

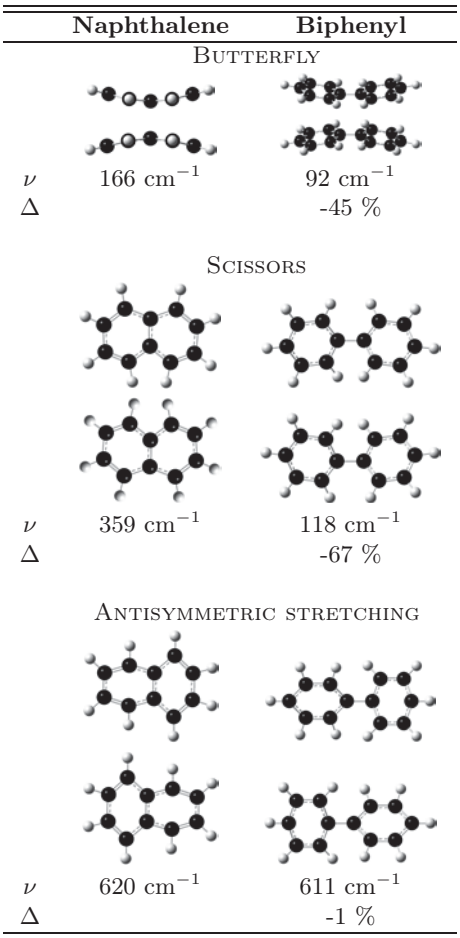

Fig. 11 Representation of the structural deformations along three low-lying vibrational modes of naphthalene and biphenyl. The influence on the vibrational frequency is emphasized.

4.2 Evolution of the butterfly mode

Due to major molecular alterations, common deformations are difficult to identify for the six molecules under scrutiny. Nevertheless, it has been possible to isolate the butterfly mode for biphenyl, diphenylmethane, bibenzyl and 2-, 3-, 4-phenyltoluene, even though no experimental observation of this mode could be strictly achieved except for biphenyl. We thus focus on the computational results obtained with the B97-1/6-311G(d,p) method. For the sake of clarity and consistency, all frequencies have been taken from the harmonic calculations. We note the great variability of this mode, predicted at 94 cm^{-1} for biphenyl (and observed at 92 cm^{-1}), 64 cm^{-1} for diphenylmethane, 47 cm^{-1} for the *gauche* bibenzyl and 54 cm^{-1} for the *anti* bibenzyl. In the case of 2-, 3-, and 4-phenyltoluene this mode is found at 43 cm^{-1}, 58 cm^{-1}, and 67 cm^{-1}, respectively. The vibrational frequency of 4-phenyltoluene is thus the closest to the corresponding mode of biphenyl, as a consequence of the terminal position of the methyl group.

5 Conclusions

Gas-phase absorption FIR spectra of biphenyl, diphenylmethane, bibenzyl and 2-, 3-, 4-phenyltoluene, six chemically related molecules containing two phenyl groups, have been recorded for the first time, allowing an accurate determination of most of their active low-frequency vibrational modes. DFT calculations have been carried out at the harmonic and anharmonic levels to assign the measured spectra of these molecules. Comparison with experimental values allows a unambiguous assignment of most observed vibrational modes.

This comparative spectral study has revealed a significant influence of the skeletal structure on the low-frequency vibrational modes of this family of molecules (with notably a sensitive dependence on the length of the interphenyl bridge) and thus illustrates once again the benefits of the FIR spectral region for discriminating species among their common structural family. Some limitations of anharmonic perturbative calculations applied to non-rigid molecules have also been emphasized. In case of bibenzyl, further efforts are currently dedicated to the issue of the eement as being caused by several possible sources. First, it is unclear whether the B97-1 method used here is sufficiently accurate to describe polyphenyl molecules. It is known that dispersion can change significantly the energetics and dynamics of molecular systems[34]. In particular, dispersion could improve the energetic stability of the *gauche* conformer with respect to the *anti* conformer and therefore increase its population at room temperature. Preliminary calculations performed using the wB97xD functional do not change the conclusions reached using other methods, but confirm the need to go beyond the perturbative treatment of anharmonicities, not only to correct for unphysical (negative) frequencies, but also to properly evaluate thermal populations. Finally, it should be kept in mind that the 2:1 ratio from calculated IR intensities has to be taken cautiously, because IR intensities are notoriously difficult to predict accurately. Additional efforts necessary to address these interesting issues require alternative appropriate tools, and will be reported in a subsequent study.

References

1 A. Léger and J. L. Puget, *Astron. Astrophys.*, 1984, **137**, L5–L8.

2 L. J. Allamandola, A. G. G. M. Tielens and J. R. Barker, *Astrophys. J.*, 1985, **290**, L25–L28.

3 K. Zhang, B. Guo, P. Colarusso and P. F. Bernath, *Science*, 1996, **274**, 582–583.

4 O. Pirali, N.-T. Van-Oanh, P. Parneix, M. Vervloet and P. Brechignac, *Phys. Chem. Chem. Phys.*, 2006, **8**, 3707–3714.

5 O. Pirali, M. Vervloet, G. Mulas, G. Malloci and C. Joblin, *Phys. Chem. Chem. Phys.*, 2009, **11**, 3443–3454.

6 M. A. Martin-Drumel, O. Pirali, Y. Loquais, C. Falvo and P. Bréchignac, *Chem. Phys. Lett.*, 2013, **557**, 53–58.

7 O. Pirali, M. Goubet, T. R. Huet, R. Georges, P. Soulard, P. Asselin, J. Courbe, P. Roy and M. Vervloet, *Phys. Chem. Chem. Phys.*, 2013, **15**, 10141–10150.

8 D. Talbi and G. S. Chandler, *J. Mol. Spectrosc.*, 2012, **275**, 21–27.

9 M. Shukla, A. Susa, A. Miyoshi and M. Koshi, *J. Phys. Chem. A*, 2008, **112**, 2362–2369.

10 G. Zerbi and S. Sandroni, *Spectrochim. Acta, Part A*, 1968, **A 24**, 483.

11 F. Cataldo, G. Angelini, A. García-Hernández and A. Manchado, *Spectrochimica Acta Part A*, 2013, **111**, 68–79.

12 M. J. Frisch, G. W. Trucks, H. B. Schlegel, G. E. Scuseria, M. A. Robb, J. R. Cheeseman, G. Scalmani, V. Barone, B. Mennucci and G. A. P. et al., *Gaussian 09 Revision A.1*, 2009, Gaussian Inc. Wallingford CT.

13 O. Bastiansen, *Acta Chem. Scand.*, 1949, **3**, 408–414.

14 Y. Takei, T. Yamaguchi, Y. Osamura, K. Fuke and K. Kaya, *J. Phys. Chem.*, 1988, **92**, 577–581.

15 H. Suzuki, *Bull. Chem. Soc. Jpn.*, 1959, **32**, 1340–1350.

16 R. M. Barrett and D. Steele, *J. Mol. Struct.*, 1972, **11**, 105.

17 L. A. Carreira and T. G. Towns, *J. Mol. Struct.*, 1977, **41**, 1–9.

18 J. G. Han, H. Xu, Z. Y. Zhu, X. H. Yu and W. X. Li, *Chem. Phys. Lett.*, 2004, **392**, 348–351.

19 W. J. D. Beenken and H. Lischka, *J. Chem. Phys.*, 2005, **123**, 144311.

20 M. Baba, Y. Kowaka, U. Nagashima, T. Ishimoto, H. Goto and N. Nakayama, *J. Chem. Phys.*, 2011, **135**, 054305.

21 I. Baraldi, E. Gallinella and M. Scoponi, *Spectrochim. Acta, Part A*, 1987, **43**, 1045–1054.

22 N. T. Hunt and S. R. Meech, *Chem. Phys. Lett.*, 2003, **378**, 195–201.

23 T. Mishra, A. K. De, S. Chattopadhyay, P. K. Mallick and P. Sett, *Spectrochim. Acta, Part A*, 2005, **61**, 767–776.

24 R. Coffman and D. S. McClure, *Can. J. Chem.*, 1958, **36**, 48–58.

25 N. R. Pillsbury, J. A. Stearns, C. W. Mueller, D. F. Plusquellic and T. S. Zwier, *J. Chem. Phys.*, 2008, **129**, 114301.

26 J. A. Stearns, N. R. Pillsbury, K. O. Douglass, C. W. Mueller, T. S. Zwier and D. F. Plusquellic, *J. Chem. Phys.*, 2008, **129**, 224305.

27 N. Kurita and P. M. Ivanov, *J. Mol. Struct.*, 2000, **554**, 183–190.

28 P. M. Ivanov, *J. Mol. Struct.*, 1997, **415**, 179–186.

29 A. Horn, P. Klaeboe, B. Jordanov, C. J. Nielsen and V. Aleksa, *J. Mol. Struct.*, 2004, **695**, 77–94.
30 M. S. Mathur and N. A. Weir, *J. Mol. Struct.*, 1972, **14**, 303.
31 A. M. North, R. A. Pethrick and A. D. Wilson, *Spectrochim. Acta, Part A*, 1974, **A 30**, 1317–1327.
32 Q. Shen, *J. Mol. Struct.*, 1998, **471**, 57–61.
33 S. Zeroual, J. Meinnel, P. Lapinski, S. Parker, A. Boudjada and A. Boucekkine, *Vibrational Spectroscopy*, 2013, **67**, 23–47.
34 T. Fornaro, M. Biczysko, S. Monti and V. Barone, *Phys. Chem. Chem. Phys.*, 2014, **16**, 10112–10128.